

Performance Study of Charcoal-based Radon Reduction Systems for Ultraclean Rare Event Detectors

M. Arthurs^a, D.Q. Huang^a, C. Amarasinghe^a, E. Miller^b and W. Lorenzon^{a*}

^a*Randall Laboratory of Physics, University of Michigan, Ann Arbor, Michigan 48109-1040, USA*

^b*SLAC National Accelerator Laboratory, Menlo Park, California 94025-7015, USA*

E-mail: lorenzon@umich.edu

ABSTRACT: The continuous emanation of radon due to trace amounts of uranium and thorium in detector materials introduces radon to the active detection volume of low-background rare event search detectors. ^{222}Rn produces as a particularly problematic background in the physics region of interest by the “naked” beta decay of its ^{214}Pb daughter nucleus. While charcoal-based adsorption traps are expected to be effective for radon reduction in auxiliary circulation loops that service the warm components of current generation 2 (G2) detectors at slow flow rates ($0.5 - 2 \text{ SLPM}$), radon reduction in the entire circulation loop at high flow rates ($\mathcal{O}(100\text{'s}) \text{ SLPM}$) is necessary to reach high sensitivity in future generation experiments. In this article we explore radon dynamics with a charcoal-based radon reduction system in the main circulation loop of time projection chamber detectors. We find that even for perfect radon traps, circulation speeds of $2,000 \text{ SLPM}$ are needed to reduce radon concentration in a 10 ton detector by 90%. This is faster by a factor of four than the highest circulation speeds currently achieved in dark matter detectors. We further find that the effectiveness of vacuum swing adsorption systems, which have been employed very successfully at reducing atmospheric radon levels in clean-rooms, is limited by the intrinsic radon activity of the charcoal adsorbent in ultra-low radon environments. Adsorbents with about ten times lower intrinsic radon activity than in currently available activated charcoals would be necessary to build effective vacuum swing adsorption systems operated at room temperature for rare event search experiments. If such VSA systems are cooled to about 190 K , this factor drops from 10 to about 2.5. This may be in reach by the time future generation experiments can be realized.

KEYWORDS: Dark Matter detectors; Time Projection Chambers; Noble liquid detectors, Liquid xenon target.

*Corresponding author.

Contents

1. Introduction	1
2. Radon Dynamics in a TPC Dark Matter Detector	2
3. Performance of a Single-Trap RRS	4
4. Swing Adsorption for Radon Reduction	9
4.1 Feasibility of Swing Adsorption RRS for Xenon	10
4.1.1 Swing Adsorption RRS with Feedback Loop and zero Intrinsic Activity	11
4.1.2 Adding a cold single trap to the Feedback Loop	13
4.1.3 Swing Adsorption RRS with non-zero Intrinsic Activity	15
4.1.4 Operating a cold VSA	17
5. Conclusion	18
A. A closer look at the single-trap in the Feedback Loop	19

1. Introduction

Radon is a radioactive noble gas that is re-supplied continuously from the decay chains of uranium and thorium present in practically every material of rare event detectors, and constitutes the dominant background source in many dark matter searches. Because radon is an inert gas, it dissolves in noble liquid detectors and cannot be removed with high temperature getters. Among the radon isotopes abundant in nature, ^{222}Rn ($\tau = 5.516$ days), a progeny of ^{238}U , is of particular concern. The beta decay of its daughter ^{214}Pb to the ground state of ^{214}Bi (6% b.r.) emits no gammas. This “naked” beta decay can end up in the low-energy region of interest for dark matter searches, survive the nuclear recoil discrimination cut, and be indistinguishable from low-energy nuclear recoils of rare particle interactions in the active volume of the detector. Discriminating against such background events is very challenging in the analysis.

Hardware mitigation is necessary to reduce the continuously re-supplied radon background for ton scale and larger noble-liquid rare event searches, including dark matter direct-detection experiments. LZ¹ is one G2 dark matter experiment [1] that addresses this need by introducing an in-line radon reduction system (iRRS) in an auxiliary circulation loop [2]. XENONnT is a different G2 dark matter experiment that employs inline distillation columns to address this need [3]. The

¹For illustration purposes we will occasionally refer to the LZ experiment, which is a generation 2, or G2, experiment with a detector mass of about 10 tons of LXe. Note, however, that the general arguments are not limited to one specific dark matter effort.

LZ iRRS, which is based on a *single* adsorption trap, takes in a small stream ($0.5 - 1$ SLPM) of radon-rich gaseous xenon from the warm regions of the xenon gas circulation system, and returns the radon-reduced xenon back to the main circulation loop. While it is expected of reducing an estimated $\mathcal{O}(20)$ mBq radon burden from the warm regions to below 1 mBq, it does not have the capacity to purify the entire 10 tons of liquid xenon.

For radon reduction of the entire system, rather than a few select areas, an iRRS in the main xenon circulation loop becomes necessary. This requires a larger trap (i.e. more adsorbent) to accommodate the much higher flow rates needed for purifying multi-ton dark matter detectors. As explored in Sec. 3, scaling up charcoal based *single-trap* radon reduction systems for multi-ton time projection chambers (TPCs) is impossible given the intrinsic radon emanation of currently-available charcoals, and impractical even if radon emanation were negligible.

Pressure swing adsorption (PSA) systems have been shown to be very effective at reducing atmospheric radon levels in clean-rooms [4]. PSA systems can generally be *multi-trap*, but are commonly employed as *two-trap* systems where the main flow of the carrier gas is alternated between the two charcoal columns allowing one column to be filled while the other is purged. Pioneering the development of PSA technology for radon reduced clean rooms, vacuum swing adsorption (VSA) systems (where the purge is at sub-atmospheric pressures) have demonstrated radon reduction efficacy of 99.7% in air at flow rates as high as 2,000 SLPM [4, 5, 6]. Section 4 explores the effectiveness of a swing adsorption system suitable for noble liquid detectors that are operated at room temperature or cooled to almost noble liquid temperature. The figures and simulations in this work are available from a public Gitlab repository [7].

2. Radon Dynamics in a TPC Dark Matter Detector

A schematic diagram of radon dynamics in a TPC detector with a RRS in the main circulation path is represented in Fig. (1). For a total radon emanation rate S in the detector, the rate of change of the number of radon atoms in the detector, N , is given by

$$\frac{dN}{dt} = -\lambda N - FN + S + r(FN), \quad (2.1)$$

where $dN_{\text{decay}}/dt = -\lambda N$ is the radon decay rate in the TPC with decay constant $\lambda = 1/\tau$; and $dN_{\text{outflow}}/dt = -FN$ is the rate of radon atoms flowing out of the TPC set by the volume exchange time T of the entire detector mass, with $T = 1/F$; and $r(FN)$ is the inflow of radon atoms that escape the RRS, with $r = N_{\text{out}}/N_{\text{in}}$ being the fraction of radon atoms escaping the RRS. For simplicity we exclude radon sources within the circulation path.

Rearranging Eq. (2.1) leads to

$$\frac{dN}{dt} = -(\lambda + F(1 - r))N + S = -\Lambda N + S, \quad (2.2)$$

which can be solved to find the total number of radon atoms

$$N(t) = -Ce^{-\Lambda t} + \frac{S}{\Lambda}, \quad (2.3)$$

where $\Lambda = \lambda + F(1 - r)$ is assumed to be constant. In Eq. (2.3), C is an integration constant defined by the initial conditions. Since we are interested in the number of radon atoms in the TPC when

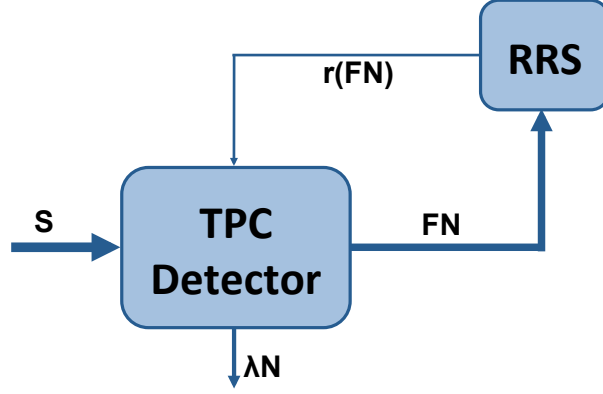


Figure 1. Schematic diagram of radon dynamics in the active volume of a dark matter detector (TPC) with a radon reduction system (RRS) in the main circulation path. Note that FN is the rate of radon atoms flowing out of the TPC; S is the radon activity in the detector; N is the number of radon atoms in the detector; and r is the fraction of radon atoms escaping the RRS.

equilibrium is reached, we can take the limit $t \rightarrow \infty$ to obtain the steady state number of radon atoms

$$N_{ss} = \frac{S}{\Lambda} = \frac{S}{\lambda + F(1-r)} = \frac{S}{\lambda + F\epsilon_{RRS}}. \quad (2.4)$$

where $\epsilon_{RRS} = 1 - N_{out}/N_{in}$, defined as the efficacy of a RRS, is a parameter that refers to the effective performance of the trap. It encapsulates both the reduction of external radon introduced to inlet of the trap, and radon emanation from the trap due to its intrinsic activity. It describes the net fraction of radon atoms removed by the trap, such that a fraction of 1 indicates a perfect trap, ie. no radon atoms emerge from the trap; a fraction of 0 indicates an ineffectual trap, ie. the same number of radon atoms enter and exit the trap; and a trap which adds more radon atoms than it removes will have a negative ϵ_{RRS} . The number of radon atoms exiting the trap is thus given by

$$N_{out} = (1 - \eta)N_{in} + N_{trap}, \quad (2.5)$$

where η is the remanent fraction of the trap, which refers to the fraction of trapped inlet radon atoms, and N_{trap} is the contribution to the trap output due to radon emanation of the trap. Combining Eq. 2.5 with the definition of efficacy leads to

$$\epsilon_{RRS} = \eta - N_{trap}/N_{in}. \quad (2.6)$$

This will be explored in greater detail in Secs. 3 and 4.

If there is no circulation at all, there will be no radon reduction. This would result in the highest possible steady state radon count in the detector,

$$N_{max} = \frac{S}{\lambda}. \quad (2.7)$$

The fractional radon reduction with a RRS is expressed by the ratio of Eqs. (2.4) and (2.7), such that

$$\frac{N_{ss}}{N_{max}} = \frac{\frac{S}{\lambda + \epsilon_{RRS}F}}{\frac{S}{\lambda}} = \frac{\lambda}{\lambda + \epsilon_{RRS}F} = \frac{\frac{1}{\tau}}{\frac{1}{\tau} + \frac{\epsilon_{RRS}}{T}} = \frac{T}{\epsilon_{RRS}\tau + T}. \quad (2.8)$$

Hence, radon reduction efficacy with a RRS in the main circulation loop of the detector, defined as $\epsilon_{Det} = 1 - N_{ss}/N_{max}$, is given by

$$\epsilon_{Det} = 1 - \frac{N_{ss}}{N_{max}} = \frac{\tau}{\tau + T/\epsilon_{RRS}}. \quad (2.9)$$

For a perfect radon reduction system ($\epsilon_{RRS} = 1$), the highest achievable radon reduction efficacy becomes

$$(\epsilon_{Det})_{max} = \frac{\tau}{\tau + T}. \quad (2.10)$$

This means that the maximum achievable radon reduction is ultimately limited by the main circulation flow rate of the detector. For LZ, with its $f = 500 \text{ SLPM}$ carrier gas flow rate resulting in a turnaround time² of about $T = 2.4$ days, and given the radon lifetime of $\tau = 5.516$ days, at most a 70% radon reduction efficacy (i.e. a radon reduction factor of 3.3) can be achieved.

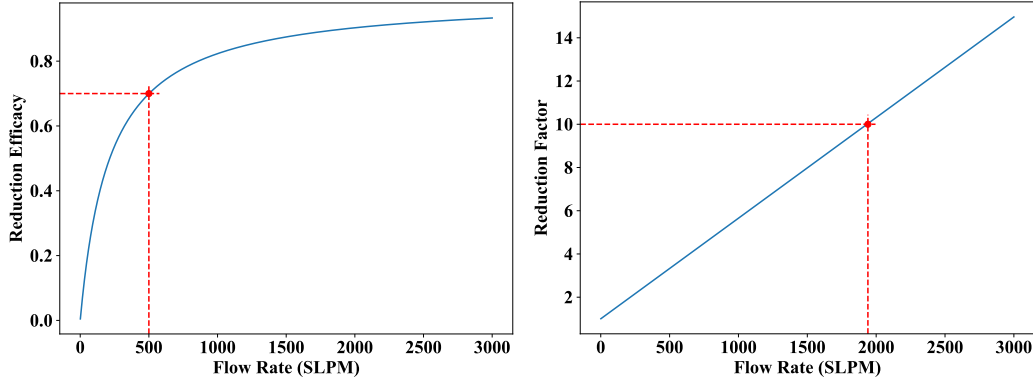


Figure 2. Left panel: maximum achievable radon reduction with a perfect radon trap in the main circulation loop for a 10-ton detector as a function of the circulation flow rate. The red dashed lines indicate the best radon efficacy achievable for the conditions at LZ. Right panel: The same data expressed in terms of the reduction factor, which has a linear relationship with the flow rate. The red dashed lines here represent the flow rate required to achieve a factor of ten reduction in radon activity.

Figure (2) shows the maximum achievable radon reduction in a TPC detector as a function of the carrier gas circulation flow rate with a perfect radon reduction system in the main circulation path of a 10-ton detector. The right panel of Fig. (2) demonstrates that in order to reach radon reduction close to 90%, flow rates of over 2,000 *SLPM* are necessary. For such high flow rates it is very challenging if not impossible with current technology to use high-temperature getters for gas purification. Purification in the liquid phase using getters, operated at cryogenic temperatures, would have to be employed similar to what has been done in very large argon TPC experiments such as ICARUS[8].

3. Performance of a Single-Trap RRS

Radon reduction in the single-trap RRS approach is accomplished by maintaining radon breakthrough times that are long enough such that the vast majority of the radon atoms entering the trap

²The turnaround time is given by $T = M/(f\rho)$, where f is the carrier gas flow rate, M is the total carrier gas mass, and ρ is the carrier gas density.

decay, while the carrier gas quickly traverses the trap. The breakthrough time of a radon atom in a charcoal trap, t_b , defined by the chromatographic plate adsorption model, is given by

$$t_b = \frac{mk_a}{f}, \quad (3.1)$$

where m is the charcoal mass, k_a is the dynamic adsorption coefficient of radon on charcoal in a carrier gas, and f is the volumetric flow rate of the carrier gas. This is an example of gas chromatography where one takes advantage of the different propagation speeds for radon and the carrier gas in the charcoal trap. The propagation speeds can vary by several orders of magnitude, particularly at cryogenic temperatures, where a ratio of $v_{Xe}/v_{Rn} = 1,000$ has been reported [9]. If the trap is big enough, so that radon needs a few lifetimes to reemerge on the other side of the trap, the overall radon concentration in the carrier gas is reduced accordingly.

For an ideal trap, i.e. a trap with negligible intrinsic activity, with a breakthrough time t_b , radon reduction is given by an exponential decay law as

$$N_{out} = N_{in}e^{-\frac{t_b}{\tau}} = N_{in}e^{-\frac{mk_a}{\tau f}} = N_{in}e^{-\frac{m}{\mu}}, \quad (3.2)$$

where N_{in} is the number of radon atoms that enter the trap and N_{out} is the number of radon atoms that emerge from the trap, and $\mu = f\tau/k_a$ represents the characteristic mass of the trap, which is the mass of charcoal, at a given flow rate, needed to reduce radon activity by a factor of e . Equation (3.2) can also be expressed in terms of input activity A_{in} and output activity A_{out} , since $A = N/\tau$, so that

$$A_{out} = A_{in}e^{-\frac{t_b}{\tau}} = A_{in}e^{-\frac{mk_a}{\tau f}} = A_{in}e^{-\frac{m}{\mu}}. \quad (3.3)$$

The amount of charcoal necessary for an ideal trap to achieve 90% efficacy as a function of flow rate of the carrier gas is shown in Fig. (3).

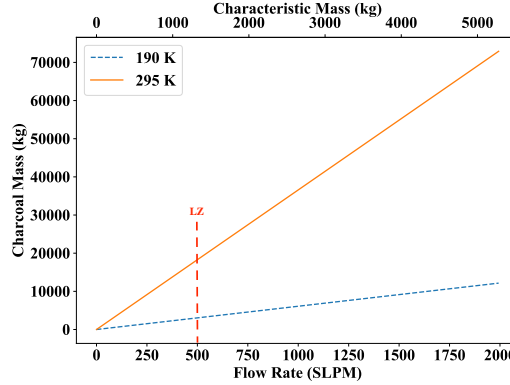


Figure 3. The amount of charcoal needed for 90% efficacy as a function of carrier gas flow rate for a single-trap RRS with zero intrinsic radon activity. The blue dashed line is at 190 K ($k_a = 3,000$ l/kg), and the orange solid line is at room temperature, 295 K ($k_a = 500$ l/kg). The dashed red line indicates the 500 SLPM carrier gas circulation flow rate in LZ.

The figure demonstrates that at the 500 SLPM nominal LZ circulation flow rate, it would take about 3,000 kg of charcoal at 190 K and 20,000 kg at 295 K to achieve a 90% radon reduction. A 3,000 kg cold trap of charcoal with a density of about 0.6 g/cm³ would occupy a volume of roughly

$5m^3$, and adsorb almost $5,000\text{ kg}$ of xenon [2]. Thus, scaling of single-traps to sustain the high flow rates needed for multi-ton dark matter experiments is not a viable option, not even for ideal traps.

At the time of writing this article, the lowest achievable intrinsic activity for commercially available synthetic activated charcoal was $\mathcal{O}(0.5\text{ mBq/kg})$ [2]. Considering that the desired radon activity after radon reduction is less than 2 mBq for the total 10 tons of xenon, the intrinsic radon activity of the charcoal cannot be ignored.

For a realistic trap, charcoal has intrinsic activity that contributes radon atoms to the output of the trap. Intrinsic activity of a charcoal is typically given by its specific activity s_o in units of mBq/kg . For a charcoal trap of mass m with specific activity s_o , the total radon activity of the trap will be ms_o (i.e. the number of radon atoms emanating from the total charcoal mass per second). Note that not all of the emanated radon atoms escape the trap — some of them decay in the trap. For a charcoal trap of a mass M ($M = v_{Rn}t_b$), assuming uniform radon emanation over the entire trap, the radon activity of a charcoal slice with length dm between m and $m + dm$ can be expressed as

$$s_o dm = \frac{A_{em}}{M} dm = A_{em} \frac{dm}{M} = A_{em} \frac{v_{Rn} dt}{v_{Rn} t_b} = A_{em} \frac{dt}{t_b}, \quad (3.4)$$

where $A_{em} = s_o M$ is the total activity of a charcoal with specific activity s_o and mass M , and dt is given by $dt = dm/v_{Rn}$. The radon contribution at the output of the trap from a such infinitesimal slice is given by

$$dA_{trap} = \frac{A_{em}}{t_b} e^{-\frac{t}{\tau}} dt. \quad (3.5)$$

Integrating Eq. 3.5 over the entire trap length gives the total radon contribution of the trap,

$$A_{trap} = \frac{s_o m}{t_b} \int_0^{t_b} e^{-\frac{t}{\tau}} dt = s_o m \frac{\tau}{t_b} \left(1 - e^{-\frac{t_b}{\tau}}\right) = s_o f \frac{\tau}{k_a} \left(1 - e^{-\frac{mk_a}{\tau f}}\right). \quad (3.6)$$

Combining Eqs. (3.3) and (3.6), the activity at the output of a single charcoal trap can be expressed as

$$A_{out} = A_{in} e^{-\frac{mk_a}{f\tau}} + s_o f \frac{\tau}{k_a} \left(1 - e^{-\frac{mk_a}{f\tau}}\right). \quad (3.7a)$$

This can be rewritten as

$$A_{out} = A_{in} e^{-\frac{m}{\mu}} + s_o \mu \left(1 - e^{-\frac{m}{\mu}}\right). \quad (3.7b)$$

Note that for sufficiently large traps, where $m \gg \mu$, the lowest achievable radon activity at the output of the trap is given by $A_{out} \approx s_o \mu$, and thus depends on the specific activity but not on the total mass of the charcoal. The temperature dependence of the characteristic mass, μ , which scales linearly with the volumetric flow rate of the carrier gas through the trap, is manifested in the temperature dependence of the adsorption coefficient k_a . For the charcoal used in the LZ iRRS [2], the adsorption coefficient increases from 500 l/kg to $3,000\text{ l/kg}$ as the temperature falls from 295 K to 190 K . This motivated the choice of the operational temperature of the LZ iRRS at 190 K , slightly above the liquefaction temperature of xenon.

Radon reduction systems based on a single-trap at cryogenic temperatures as low as 190 K are very effective at flow rates of $0.5 - 1\text{ SLPM}$, and require relatively small amounts of charcoal. The LZ experiment utilizes such an approach to reduce by more than 90% the radon contribution from the warm parts of the detector with a 10 kg trap made of Saratech [2] synthetic charcoal. In

the remainder of this section, the performance of a single-trap RRS is explored in terms of RRS efficacy, which encapsulates both, the reduction of the inlet activity, as well as the contribution from the intrinsic activity of the charcoal.

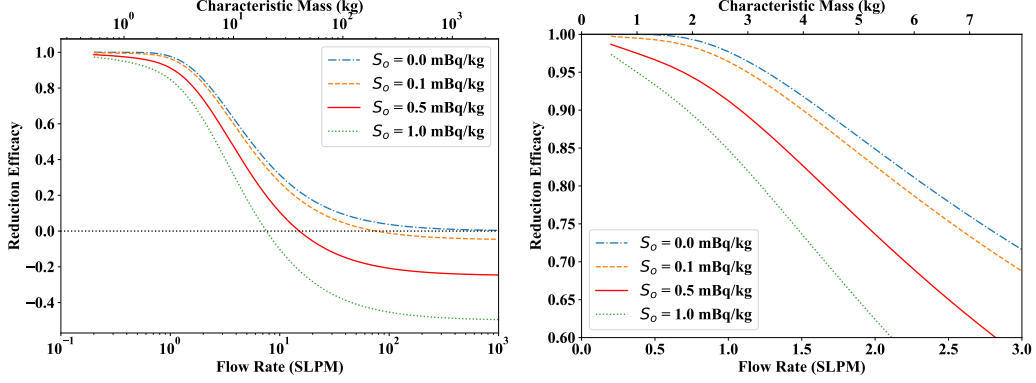


Figure 4. Left panel: efficacy of a 10 kg charcoal single trap with dynamic adsorption coefficient of $k_a = 3,000 \text{ l/kg}$ (at 190 K), total inlet radon activity of $A_{in} = 20 \text{ mBq}$ as a function of the flow rate of the carrier gas for a various intrinsic radon activities s_o . Right panel: zooms in to flow rates below 3 SLPM. The solid red curve corresponds to specific radon activity of the charcoal used in the LZ iRRS, which is the best commercially affordable candidate.

The efficacy of a 10 kg charcoal trap is about 90% or higher for flow rates below 1 SLPM in the range of 0 – 1.0 mBq/kg specific activities of charcoal, as seen on the right panel of Fig. (4). However, the efficacy rapidly falls and even becomes harmful for flow rates above 15 SLPM, as seen on the left panel of Fig. (4). Even for an ideal charcoal with zero intrinsic activity, the efficacy of the trap rapidly falls at flow rates above 3 SLPM.

Note that the efficacy of the trap, $\varepsilon = 1 - A_{out}/A_{in}$, depends on the input radon activity. Expressed in terms of Eq. (3.7b), the trap efficacy can be expressed as

$$\varepsilon = 1 - A_{out}/A_{in} = 1 - e^{-\frac{m}{\mu}} - \frac{s_o \mu}{A_{in}} \left(1 - e^{-\frac{m}{\mu}}\right) = \left[1 - \frac{s_o \mu}{A_{in}}\right] \left(1 - e^{-\frac{m}{\mu}}\right). \quad (3.8)$$

Figure (4) uses a value of 20 mBq, which is the input radon activity A_{in} into the RRS expected for the LZ detector. The relevant parameter for the efficacy of a RRS is the ratio of the specific activity of the charcoal and the input radon activity, present in the efficacy definition as $(s_o \mu / A_{in})$. Note that the efficacy of a given adsorptive trap increases for an increasing input radon activity. This makes the technique particularly well-suited for radon reduction from radon-rich environments.

Figure (5) explores trap efficacy for a specific activity fixed at 0.5 mBq/kg as a function of flow rate of the carrier gas, for a range of charcoal masses between 5 – 100 kg. For flow rates below 15 SLPM, where radon contribution from the charcoal is smaller than radon reduction due to adsorption, a greater mass of charcoal results in a higher efficacy, as shown in the right panel.

The inflection point in the left panel occurs at a flow rate where the radon contribution from the charcoal compensates the reduction due to adsorption. At this critical flow rate, which is about 15 SLPM for an input activity of 20 mBq and a specific radon activity of 0.5 mBq/kg, the ratio $s_o \mu / A_{in}$ is unity, the exponential terms in Eq. (3.7b) cancel, and the efficacy of the trap becomes

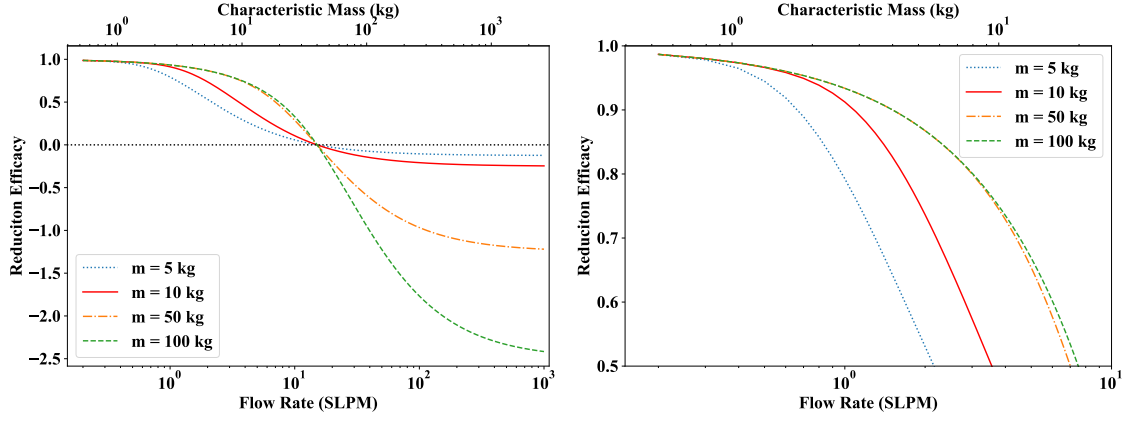


Figure 5. Left panel: efficacy of a charcoal single trap with dynamic adsorption coefficient of $k_a = 3,000 \text{ l/kg}$ (at 190 K), intrinsic radon activity $s_o = 0.5 \text{ mBq/kg}$ and a total inlet radon activity of $A_{in} = 20 \text{ mBq}$ as a function of the flow rate of the carrier gas. The various curves represent efficacies for different masses of charcoal. The solid red curve corresponds to 10 kg mass as in the LZ iRRS. Right panel: zooms in to flow rates below 10 SLPM .

zero. Above this flow rate, the efficacy becomes negative indicating that the radon reduction system becomes harmful and introduces more radon atoms to the detector than it removes.

The right panel of Fig. (5) shows that for the given characteristic parameters of the charcoal (such as s_o and k_a), the efficacy of 50 kg and 100 kg traps are very similar at flow rates below 10 SLPM . This indicates that for a given specific activity and adsorptive property of a charcoal there is an effective mass above which the efficacy of the trap is not improved significantly, as long as the flow rates are small enough such that the radon contributions from the trap are not dominant.

For flow rates below the critical value, the maximal efficacy of a trap is obtain from the limit of $m \rightarrow \infty$ and is expressed as

$$\varepsilon_{max} = 1 - (A_{out})_{m \rightarrow \infty} / A_{in} = 1 - \frac{s_o \mu}{A_{in}} = 1 - (s_o / A_{in})(f \tau / k_a). \quad (3.9)$$

which leads to the expression for the trap efficacy of

$$\varepsilon = \varepsilon_{max} \left(1 - e^{-\frac{m}{\mu}}\right). \quad (3.10)$$

Figure (6) shows the dependence of ε_{max} as a function of flow rate, for specific charcoal activities in the range of $0.001 - 0.5 \text{ mBq/kg}$. It turns out that for a single-trap RRS to be effective at flow rates close to the nominal LZ main circulation flow rate of 500 SLPM , adsorbents with intrinsic radon activity of $10 \mu\text{Bq/kg}$ or lower are necessary. The lowest commercially available activated charcoal is $\mathcal{O}(0.5) \text{ mBq/kg}$ [2], about two orders of magnitude greater than what is needed.

For flow rates below the critical flow rate, the efficacy of the trap increases with increasing charcoal mass, and it rapidly approaches its maximal value. Figure (7) shows the efficacy of a single trap as a function of charcoal mass for a fixed intrinsic radon activity of 0.5 mBq/kg , and a constant total input radon activity of 20 mBq in a range of $0.5 - 20 \text{ SLPM}$ flow rates of the carrier gas. As expected, at a flow rate of 15 SLPM , the efficacy of the trap is independent of the mass of charcoal in the trap and is always zero. Furthermore, above some effective charcoal mass

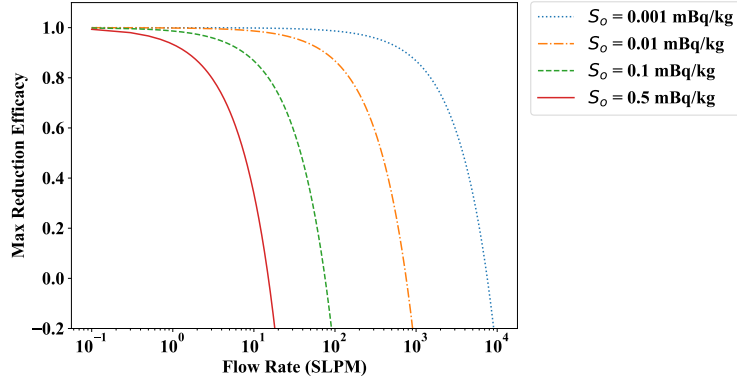


Figure 6. Maximum achievable radon reduction of a single-trap in the main circulation loop of a TPC detector as a function of the circulation flow rate. A dynamic adsorption coefficient of charcoal $k_a = 3,000 \text{ l/kg}$ (at 190 K) and a total inlet radon activity $A_{in} = 20 \text{ mBq}$ is assumed. The various curves represent different intrinsic radon activities of charcoal. The solid red curve corresponds to the intrinsic radon activity of Saratech charcoal used in the LZ iRRS.

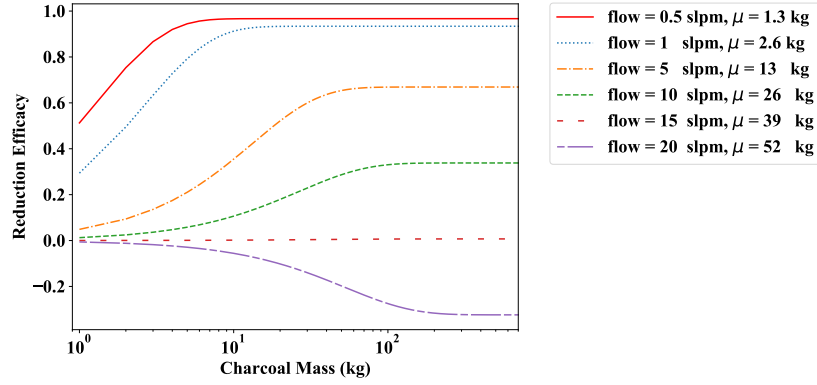


Figure 7. Efficacy of single column charcoal trap with dynamic adsorption constant $k_a = 3,000 \text{ l/kg}$ (at 190 K), intrinsic radon activity $s_o = 0.5 \text{ mBq/kg}$, and a total inlet radon activity of $A_{in} = 20 \text{ mBq}$ as a function of the charcoal mass. The various curves represent different flow rates and their corresponding characteristic masses μ . The solid red curve corresponds to the nominal 0.5 SLPM flow rate through the LZ iRRS.

(approximately 4μ), the increase in the efficacy is asymptotically small. Assuming a fixed total input radon activity of 20 mBq , at the nominal LZ iRRS flow rate of 0.5 SLPM (red solid curve), the effective mass of the the trap is slightly over 7 kg of charcoal, where it reaches its maximum efficacy of over 95%. Similarly at higher flow rates, yet less than 15 SLPM, maximum efficacy is reached with charcoal masses ranging from 10 – 100 kg.

4. Swing Adsorption for Radon Reduction

Vacuum swing adsorption (VSA) systems have been developed for radon reduction in clean rooms for flow rates of order 1,000 SLPM. This is in contrast to single-trap radon reduction systems whose performance is set by the steady-state radon output, which limits the flow rate. VSA systems are

based on multi-trap systems — typically consisting of two charcoal columns — where the flow direction of the carrier gas is switched between the columns.

A schematic view of a VSA system for radon reduction in air is presented in Fig. (8). Ambient air is fed into column 1 (here the feed column) for a time much shorter than the time required for radon atoms to transit the column, while column 2 (here the purge column) is purged with a small stream of radon-reduced air from the outlet end of column 1³ to flush the radon atoms out. At the end of this cycle, column 2 has been regenerated and is ready to be fed with outside air, while column 1 has accumulated radon and is ready to be purged. With the beginning of the next cycle, the outside air is directed into column 2 (now the feed column), while column 1 (now the purge column) is purged. By the end of the second cycle, each column has gone through one feed and one purge cycle. The time required to complete these two cycles is typically called a swing-cycle period.

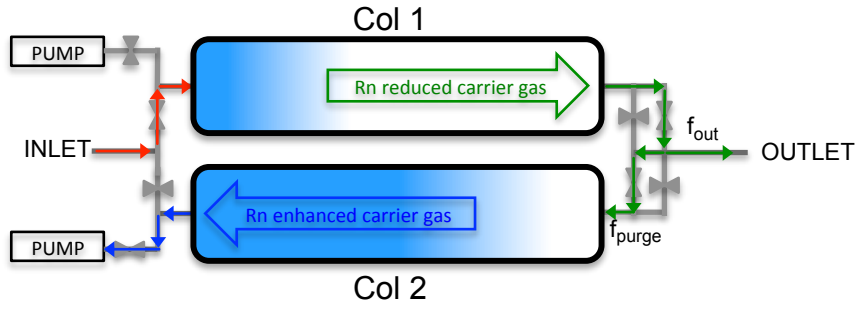


Figure 8. A schematic view of a VSA system for radon reduction in air. Flow of the input air is alternated between columns 1 and 2 to prevent radon escaping from the outlet ends of the columns. While one column is fed with air, the other is purged with a small stream of radon-reduced air. The shades of blue indicate the radon concentrations in the two columns, the red arrows indicate the flow of the input gas, the green arrows indicate the flow of the radon-reduced output gas, and blue arrows indicate the pump-out flow.

By switching a given flow between the two columns, each column may be much smaller than the column in a single-trap RRS. Unlike in single-trap reduction systems, where radon atoms are retained in the charcoal for many lifetimes, in a swing system they are flushed out of the system before most have a chance to decay. Additionally, unlike single-trap reduction systems, which are typically cooled down to cryogenic temperatures, VSA systems are shown to reach high efficacy even at room temperature. Over the past decade, VSA technology has been improved to reach radon reduction efficacy in air of greater than 99.9% [5, 6]. For an inlet radon activity of about 80 Bq/m^3 , reduction factors of greater than 1,000 were achieved, reducing the clean room radon activity down below the sensitivity of the RAD7 measurement device, with an upper limit of 0.067 Bq/m^3 [6].

4.1 Feasibility of Swing Adsorption RRS for Xenon

Considering the great success of VSA systems for radon-reduced clean rooms, we will now explore the viability of such a system for full scale radon reduction in a rare-event TPC detector, taking into account some distinct differences.

³Typically approximately 10% of the radon-reduced air emerging from the outlet of the feed column is used for purging the radon-enhanced column while a vacuum pump maintains the column pressure around 10 mBar.

Since the radon content introduced to a VSA system due to the intrinsic activity of charcoal is typically much smaller than that in atmospheric air, it is mostly ignored in VSA systems used for radon reduction in clean rooms. Conversely, in a liquid xenon dark matter detector with a radon content as low as 1 atom/kg of xenon, the introduction of a charcoal trap could very well introduce more radon than it removes. For simplicity, we will start with ignoring intrinsic activity (Sec. 4.1.1), and then study the impact of non-zero intrinsic activity on VSA systems (Sec. 4.1.3).

Furthermore, in contrast to air purification systems, where the purged air is released back into the atmosphere, xenon is expensive, and needs to be captured and returned to the purification system, as shown schematically in Fig. (9). Therefore, rather than pumping and releasing the xenon gas into atmosphere, the radon-rich purge gas has to be returned to the inlet of the swing system. In such a system, the radon atoms become effectively trapped and accumulate in the feedback loop. Accumulation of radon atoms in the feedback loop continues until it is balanced by the decay of the radon atoms and steady state is reached. Note that such a system conveniently provides a mechanism for radon atoms to decay outside of the TPC detector.

Because of the cyclic nature of the swing system, its columns never reach steady state. The full modeling of the system is therefore more involved and must track radon concentrations throughout each column and propagate them over time. The exact behavior will depend strongly on the choice of charcoal [2], the geometry of the columns, the pumping speed of the system, and other system-dependent properties. While this system-dependent modeling is beyond the scope of this work, models prepared for other systems have shown that radon appearing at the VSA output is primarily due to the long diffusive tail of the radon front as it propagates through the charcoal [4]. Thus, the remanent fraction of the VSA will depend on the elution curve of radon in the trap as well relative values of the cycle time and the trap breakthrough time. For simplicity, we fold this into a single constant remanent fraction for the feed column when modeling the performance of the VSA.

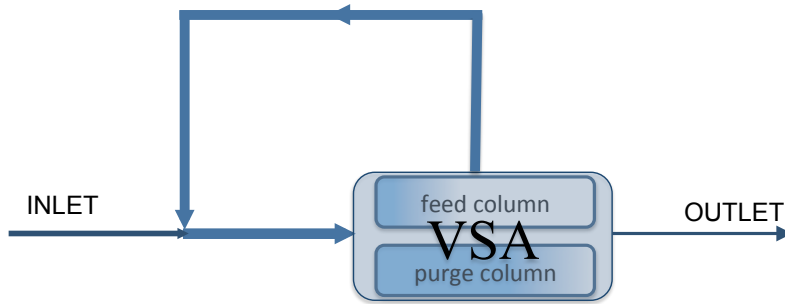


Figure 9. A schematic view of a VSA system with a feedback loop for radon reduction in xenon. Flow of the input xenon is alternated between the two columns, but unlike in a radon reduction system for air, where the purged air is released back into the atmosphere, the purged xenon is returned through a feedback loop to the inlet of the VSA.

4.1.1 Swing Adsorption RRS with Feedback Loop and zero Intrinsic Activity

In order to evaluate steady state conditions for a VSA system with a feedback loop, let us consider the dynamics of radon atoms in a single cycle. For simplicity, and to compare with radon reduction

systems in clean rooms, we will start with ignoring intrinsic radon activity. Let us consider the situation where some radon atoms entering at the inlet are allowed to escape the VSA system.

In this specific model the feed column remanent fraction, η_{feed} , represents the fraction of input radon atoms being trapped in the feed column of the VSA. After the n^{th} feed of the VSA,

$$(N_{out})_n = (N_{in})_n(1 - \eta_{feed})f_{out}, \quad (4.1a)$$

and

$$(N_{in})_{n+1} = N_{det} + (N_{in})_n(1 - \eta_{feed})f_{purge} + (N_{loop})_n, \quad (4.1b)$$

where N_{out} is the number of radon atoms that emerge from the VSA and make it back to the TPC detector; N_{in} is the number of radon atoms that enter the feed column, which contains both the constant supply from the detector N_{det} , as well as the radon atoms from the feedback loop; f_{out} is the fraction of the radon-reduced carrier gas that flows out of the feed column and back to the TPC detector; $f_{purge} = 1 - f_{out}$ is the fraction of the radon-reduced carrier gas that is used for purging the radon-enhanced purge column; and T_{feed} is the time that a VSA column is in the feed stage, which must be less than the breakthrough time, t_b , of the column to avoid radon atoms starting to escape from that column.

The first term in Eq. (4.1b) represents the constant radon input from the detector. The second term represents the radon atoms that escaped the feed column and are reintroduced into the purge column by the purging process. The third term in Eq. (4.1b),

$$(N_{loop})_n = (N_{in})_n \eta_{feed} e^{-\frac{T_{feed}}{\tau}}, \quad (4.2)$$

represents the radon atoms that were trapped in the VSA columns and returned to the VSA inlet through the feedback loop. Specifically, it is the number of radon atoms that did not decay in the column during the *feed stage*. Radon breakthrough time in the feed column is about an order of magnitude greater compared to the breakthrough time in the purge column. The mass flow rate of the purge flow is (1/10) of the feed flow, but the purge pressure is (1/100) of the feed pressure, resulting into a 10 times larger volumetric flow rate ($f \propto P\phi$), where ϕ is the mass flow rate, f is the volumetric flow rate and P is the pressure) [4]. Thus the breakthrough time of the purge column is (1/10) of the feed column. Therefore, the decay of radon atoms in the purge column is neglected.

As an example, the left panel of Fig. (10) illustrates that the steady state fraction of radon atoms escaping a feed column, $r_{ss} = (N_{out})_{ss}/N_{det}$, with remanent fraction of 99%⁴ that uses a 10% purge flow fraction, varies between 0.7 and 0.1 with feed cycle times between 30min and 600min, respectively. The right panel of Fig. (10) demonstrates that up to 300 feed cycles are necessary to reach steady state (with $r_{ss} = 0.55$) for feed cycle times of 60min.⁵ Although not explicitly shown here, fewer feed cycles are needed to reach steady state as the feed cycle times get longer.

⁴For a feed column with remanent fraction of 99% , 1% of the radon atoms entering the trap are allowed to escape it, while the other 99% remain in the trap.

⁵For a VSA column of mass $m = 90kg$, adsorption coefficient $k_a = 500l/kg$, and flow rate of $f = 500 SLPM$, the breakthrough time $t_b = k_a m / f$ is 90min. The feed cycle time of the VSA column is chosen to be $T_{feed} = t_b / 1.5 = 60min$ to avoid leakage of radon atoms from the VSA columns. The factor of 1.5 appears sufficient for Saratech charcoal [2], and 60min is typical for radon-reduction clean room VSA systems [6].

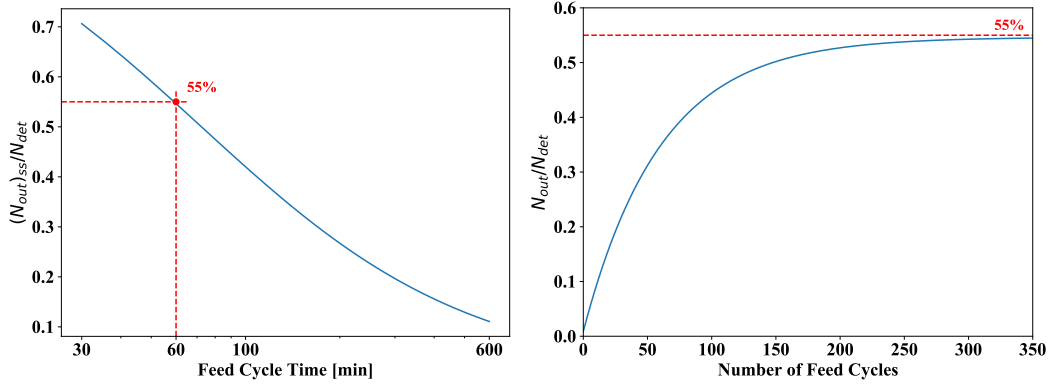


Figure 10. Dynamics of radon atoms in a VSA system with a feedback loop for $\eta_{feed} = 0.99$, charcoal mass $m = 90\text{ kg}$, adsorption coefficient $k_a = 500\text{ l/kg}$, and flow rate $f = 500\text{ SLPM}$, operated at room temperature. Left panel: steady state fraction of radon atoms escaping the VSA versus feed time for xenon purification. The fraction drops exponentially over a large variation of feed cycle times. Right panel: fraction of radon atoms escaping the trap versus the number of feed cycles for a feed cycle time of 60 min , as indicated with the dashed lines in the left panel. It takes about 300 feed cycles to approach steady state ($r_{ss} = 0.55$) in the VSA, assuming a constant influx of radon atoms from the TPC detector.

Figure (10) has shown that in order to increase steady state radon reduction efficacy in a VSA system, defined as $\epsilon_{RRS} = 1 - r_{ss}$, one can increase the feed cycle time. This requires very large charcoal columns, since the breakthrough time, which must be larger than the feed cycle time, grows linearly with charcoal mass. This is exacerbated in xenon-based TPC detectors, since the radon adsorption coefficient k_a in xenon carrier gas (500 l/kg) is about ten times smaller [2] than in air or even in argon carrier gas ($5,400\text{ l/kg}$). This does not only increase the cost associated with the increased trap size, but also the amount of xenon stored in the charcoal, which is about 0.4 kg/kg at room temperature [2], and can become a significant fraction of the entire xenon mass.

Note, the assumption of a feed column with remanent fraction 99% may be optimistic. Relaxing that number to a conservative value of 90% will reduce the steady state RRS radon reduction efficacy from 45% to 7%.

4.1.2 Adding a cold single trap to the Feedback Loop

An improvement is to integrate a single-trap RRS, which is preferably cooled, in the feedback loop of the VSA system, shown schematically in Fig. (11), such that the radon-enhanced gas from the purge column passes through the single-trap RRS before it is fed back into the inlet of the VSA. Such a trap provides a space for radon atoms to decay before being returned to the VSA. In such a system, only a small fraction (say 10%) of the entire carrier gas circulation volume has to pass through the single-trap RRS. In addition, we will show that this trap can have a relatively low efficacy while still significantly improving the performance of the system.

The addition of a single-trap in the VSA feedback loop can be implemented in the radon dynamics model with a small modification in Eq. (4.1b), so that

$$(N_{in})_{n+1} = N_{det} + (1 - \epsilon_{st}) [(N_{in})_n (1 - \eta_{feed}) f_{purge} + (N_{loop})_n], \quad (4.3)$$

where ϵ_{st} is the efficacy of the single trap and N_{loop} is defined by Eq. (4.2).

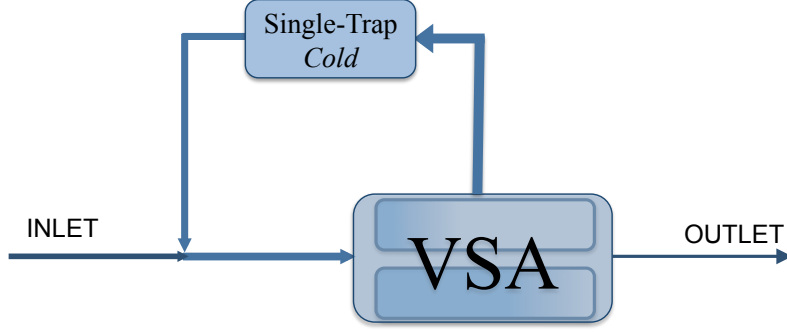


Figure 11. A schematic of a VSA system with a single, cold trap in the feedback loop for radon reduction in xenon. The cold trap greatly enhances the efficacy of the VSA system.

A map of the RRS efficacy as a function of single-trap efficacy and feed column remanent fraction is shown in Fig. (12). It shows that the feed column remanent fraction needs to be 90% or higher, while the single-trap efficacy needs to be at least 10% to reach a RRS efficacy of at least 50%. For illustration purposes, let us consider an example that integrates a single-trap with an efficacy of only 10% in the feedback loop of a VSA with a feed column remanent fraction of 90%, shown as white dashed lines Fig. (12). A steady state RRS efficacy of 52% is reached, which corresponds to an improvement of about a factor of 5 over a VSA system without a single-trap of modest efficacy.

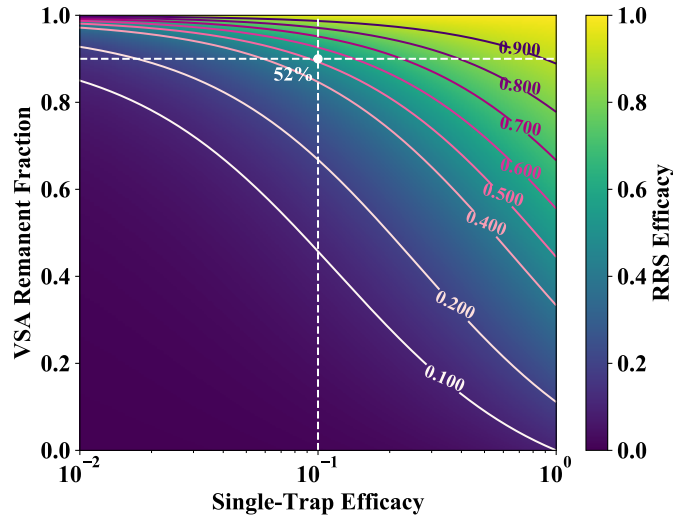


Figure 12. Radon reduction efficacy as a function of single-trap efficacy and VSA feed column remanent fraction. The white point indicates about 52% radon reduction efficacy as a result of a single-trap with 10% efficacy in the feedback loop of a feed column with remanent fraction of 99%.

Based on Eq. (2.9) in Sec. (2), radon reduction within a TPC detector, such as LZ, can be computed for a given efficacy of the RRS. For the 52% efficacy considered in the example, the radon reduction efficacy within LZ is calculated to be 55%, which is approaching the maximal 70% achievable with a perfect RRS system. The steady state radon reduction performance within

the TPC detector with a swing adsorption system in the main circulation path, as a function of radon fraction escaping the single trap ($1 - \epsilon_{st}$) and radon fraction escaping the VSA ($1 - \eta_{feed}$) is shown in Fig. (13).

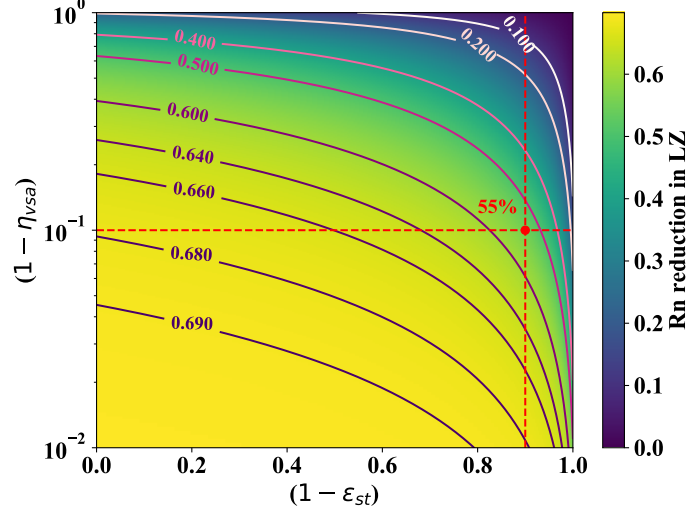


Figure 13. Radon reduction within a TPC detector, such as LZ (ϵ_{TPC}) with a single-trap swing adsorption RRS in the main circulation path of a VSA system as a function of both the radon fraction escaping the single-trap ($1 - \epsilon_{st}$) and the feed column ($1 - \eta_{feed}$). The red point indicates about 55% radon reduction in the TPC detector with a RRS of 52% efficacy.

Thus it appears that introducing a single trap, even with modest efficacy, in the feedback loop of a VSA system seems feasible, if the intrinsic radon activity of the activated charcoal can be ignored. Details for how to design a single trap with 10% efficacy in a feedback loop are discussed in Appendix A.

4.1.3 Swing Adsorption RRS with non-zero Intrinsic Activity

Radon levels desired in a dark matter detector are about 5 orders of magnitude lower ($\mathcal{O}(1 - 2) \mu\text{Bq/kg}$) than those required in radon-reduced clean-rooms ($\mathcal{O}(100) \text{mBq/kg}$). It is therefore not realistic to assume that the intrinsic activity of the charcoal can be ignored. In Eqs. (4.1a) and (4.3), which describe the evolution of radon counts in an adsorption swing system, N_{in} and N_{out} correspond to the radon input and output in a single feed cycle. Thus we need to find the number of radon atoms introduced to the VSA due to emanation from the charcoal in a feed cycle. The total radon activity of a trap, A_{trap} , with breakthrough time t_b , is given by Eq. (3.6), which is the steady state radon contribution taking into account self adsorption of radon atoms that have been emanated deeper in the trap. However the number of radon atoms introduced to the VSA by the trap is not a steady state contribution since the flow through a VSA column is not continuous. The radon contribution from the trap in a feed cycle can be expressed as

$$(N_{trap})_{feed} = \int_0^{T_{feed}} dt \int_0^{t_b} dt' \frac{s_o m}{t_b} e^{-\frac{t'}{\tau}} H(t - t') = \int_0^{T_{feed}} dt \int_0^t dt' \frac{s_o m}{t_b} e^{-\frac{t'}{\tau}}, \quad (4.4)$$

where $H(t - t')$ is the Heaviside step function, which enables to include only the radon contribution from the part of the trap that had enough time to reach the outlet. Therefore the trap contribution in a single feed cycle is obtained from Eq. (4.4) to be

$$(N_{trap})_{feed} = \tau^2 \frac{s_o m}{t_b} \left[e^{-\frac{T_{feed}}{\tau}} - \left(1 - \frac{T_{feed}}{\tau} \right) \right], \quad (4.5)$$

which can be approximated to

$$(N_{trap})_{feed} \approx \frac{s_o m}{2t_b} T_{feed}^2.$$

This approximation is valid since the feed cycle time of the VSA is much shorter than the radon lifetime ($T_{feed} \ll \tau$), and will always over-estimate radon content. Equation (4.5) can be added to Eqs. (4.1a) and Eq. (4.3) such that

$$(N_{out})_n = (N_{in})_n (1 - \eta_{feed}) f_{out} + (N_{trap})_{feed} f_{out}, \quad (4.6a)$$

and

$$\begin{aligned} (N_{in})_{n+1} = N_{det} + (1 - \epsilon_{st}) & \left[(N_{in})_n (1 - \eta_{feed}) f_{purge} \right. \\ & + (N_{loop})_n \\ & \left. + (N_{trap})_{feed} f_{purge} + (N_{trap})_{purge} \right]. \end{aligned} \quad (4.6b)$$

The second term of Eq. (4.6a), $(N_{trap})_{feed} f_{out}$, represents the number of radon atoms emanated from the charcoal in the feed column that flow into the TPC detector. In the last line of Eq. (4.6b), $(N_{trap})_{feed} f_{purge}$ represents the radon contribution introduced by the purge flow which originated in the feed column, and $(N_{trap})_{purge}$ represents the radon contribution from the purge column. By design, the purge column has about an order of magnitude shorter breakthrough time compared to the feed column as discussed in Sec. 4.1.1, which leads to less self adsorption of emanated radon atoms during the purge process, thus increases its radon contribution due to emanation. Therefore, the contribution from the feed column is much smaller than the contribution from the purge column.

Let us continue with the example illustrated in Sec. 4.1.1, where we integrated a single-trap of 0.1 efficacy in the feedback loop of a VSA with a feed column that has 0.9 remanent fraction. As mentioned earlier, in our model the intrinsic activity of the VSA columns is treated separately and the parameter η_{feed} does not take into account the non-zero radon activity introduced by charcoal. However we can now estimate the total efficacy of the RRS considering non-zero intrinsic charcoal activity. The number of input radon atoms in one feed cycle time is $(N_{det})_{feed} = \rho_{Xe} s_{Xe} f T_{feed} \tau = (0.356 \text{ mBq/feed}) \tau$, assuming a radon activity s_{Xe} of $2 \mu\text{Bq/kg}$ in xenon, a xenon density of $\rho_{Xe} = 5.86 \text{ g/l}$, and a flow rate of $f = 500 \text{ SLPM}$.

The left panel of Fig. (14) shows that charcoal with specific activity near $s_o = 0.03 \text{ mBq/kg}$ or less is needed to achieve a radon reduction efficacy of 40% for an inlet radon activity of $2 \mu\text{Bq/kg}$. This is about a factor of ten lower than the activities of currently available adsorbents. Note that if the inlet radon activity is higher, the RRS will have higher efficacy. This is illustrated in the left panel of Fig. (14) with the orange dotted curve for $s_{Xe} = 5 \mu\text{Bq/kg}$, where the RRS efficacy is about 48% for a specific activity near $s_o = 0.03 \text{ mBq/kg}$. This is close to the highest efficacy (52%) achievable with negligible intrinsic charcoal activity. The right panel of Fig. (14) shows

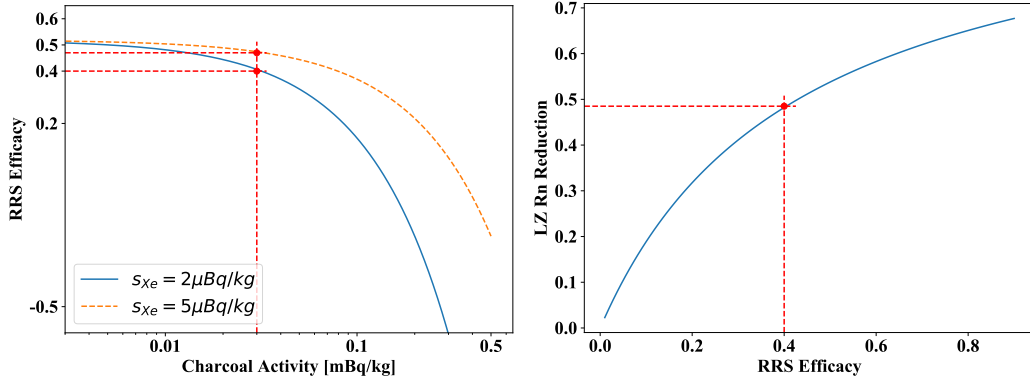


Figure 14. Left panel: Swing adsorption RRS efficacy as a function of specific charcoal activity for the example considered in Sec. 4.1.1. That system integrates a single-trap of efficacy $\epsilon_{st} = 0.1$ in the feedback loop of a VSA with $\eta_{feed} = 0.9$ feed column. The blue solid curve is for inlet radon activity of $2 \mu\text{Bq/kg}$, and the orange dotted curve is for inlet radon activity of s_{Xe} of $5 \mu\text{Bq/kg}$. The red dashed lines are explained in the text. Right panel: radon reduction efficacy in LZ as a function of RRS efficacy that is in the main circulation path.

radon reduction efficacy in LZ as a function of the efficacy of a RRS on the main circulation path. As seen, a RRS with 40% efficacy would result in almost a factor of 2 radon reduction in LZ.

4.1.4 Operating a cold VSA

So far, VSA operation has only been considered at room temperature (ie. 295 K). However, because the adsorption coefficient of charcoal increases with decreasing temperature following the Arrhenius Law [2], cooling the VSA down to 190 K shows considerable promise. As shown in Fig. (15),

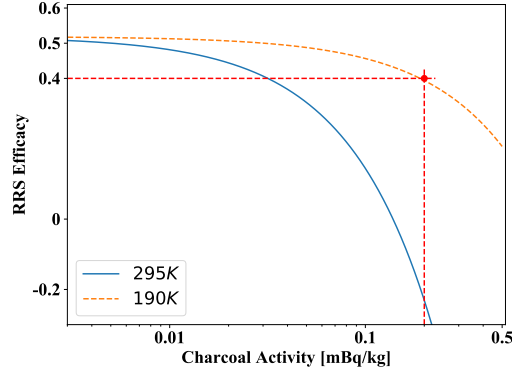


Figure 15. Efficacy of a swing adsorption RRS as a function of specific charcoal activity for an inlet radon activity of $2 \mu\text{Bq/kg}$ for the specific example considered in Sec. 4.1.1. That system integrates a $\epsilon_{st} = 0.1$ efficacy single-trap in the feedback loop of a VSA with remanent fraction $\eta_{feed} = 0.9$. The blue solid curve represents the efficacy of the RRS when the VSA is cooled down to 190 K and the dashed orange curve is at VSA operational temperature of 295 K .

the efficacy of the cooled VSA system becomes comparable to that of a VSA system operated at room temperature, but with significant relaxation on the demand for intrinsic charcoal activity. In

fact, the demand relaxes by almost an order of magnitude, which may be in reach by the time future generation experiments can be realized [10].

Specifically, at room temperature, a trap with 90 kg of charcoal and an adsorption coefficient k_a of 500 l/kg has a breakthrough time of 90 min, while at 190 K the adsorption coefficient is $k_a = 3,000$ l/kg [2]. For a breakthrough time of 90 min, the six times larger adsorption coefficient allows the mass to be 15 kg instead of 90 kg, significantly reducing the radon contribution from emanation from the trap. The efficacy of such an RRS with a single-trap in the feedback loop and an inlet radon activity of $2 \mu\text{Bq/kg}$ becomes about 40% for an intrinsic charcoal activity of 0.2 mBq/kg . This is only a factor of 2.5 lower than that of Saratech, the charcoal used in the LZ iRRS. This is in stark contrast to a VSA operated at room temperature which would be harmful (i.e. introduces more radon than it removes) for the same charcoal.

5. Conclusion

Radon and its daughters constitute the most significant backgrounds in rare event searches since they are continuously resupplied from detector materials. Although radon screening of every single detector component is vital to reach high sensitivity for dark matter detection, it is not sufficient. Further mitigation strategies are required that include both, in-situ hardware radon reduction and background discrimination in the analysis of the data.

The performance of charcoal-based radon reduction systems has been explored. For illustration purposes, references to the LZ detector have been made, but the general arguments and observations are not limited to one specific dark matter experiment. In-line radon reduction systems in auxiliary circulation loops, as employed in the LZ experiment, reduce radon-rich gaseous xenon from the warm components of the detector before they return radon-reduced xenon back to the main circulation loop. This single, charcoal-based, adsorption trap approach is effective for slow circulation flow rates, but breaks down at high circulation flow rates, which are required to purify entire volumes of ton scale or larger noble-liquid detectors. It is found that scaling up charcoal-based single-trap radon reduction systems, to make them viable at the circulation flow rates of multi-ton TPC detectors, is impractical even if radon emanation from charcoal is negligible.

Vacuum swing adsorption systems, which have shown great success at reducing atmospheric radon levels in clean-rooms, have clear advantages over single-trap systems. They need to be modified so that they can capture and return the noble carrier gases to the purification system through a gas feedback loop rather than releasing them into the atmosphere. The drawback of such systems is that the radon atoms become effectively trapped and can lead to many-fold higher radon concentrations in the feedback circulation loop. This can be ameliorated by introducing a modest cold single-trap into the feedback loop. It allows the radon atoms to accumulate and decay in the single trap, rather than in the charcoal columns of the swing adsorption system, where some fraction can escape and be reintroduced into the TPC detector. It is found that for a VSA system with a feed column of 0.9 remanent fraction, introduction of even a 0.1 efficacy single trap in the feedback loop improves the overall radon reduction efficacy from about 7% to over 50% (intrinsic activity of charcoal is ignored in this example).

While this is encouraging, it needs to be pointed out that VSA systems too are limited by the intrinsic radon activity of their charcoal adsorbent, particularly if they are operated at room

temperature. Under these circumstances, adsorbents with about a factor of ten lower intrinsic radon activity than in currently available activated charcoals are required to build effective vacuum swing adsorption systems for rare event search experiments. If such VSA systems are instead cooled to about 190K, this factor drops from 10 to about 2.5, which may be in reach by the time future generation experiments can be realized. Other options, not pursued here, might include radon purification in the liquid phase.

Acknowledgments

We acknowledge support of the U.S. Department of Energy (DOE) Office of Science under grant numbers DE-SC0015708 and DE-SC0019193, and under contract number DE-AC02-76SF00515, the SLAC National Accelerator Laboratory and the University of Michigan. We would like to thank Dr. Richard Raymond at the University of Michigan for many helpful conversations. We would also like to thank the members of the LZ collaboration for many insightful discussions.

A. A closer look at the single-trap in the Feedback Loop

The example of a VSA system with 90% remanent fraction, discussed in Sec. 4.1.2, included a cold, single-trap in the feedback loop. It was assumed that this single trap had a modest efficacy of 10%, and that it could support a 50 *SLPM* flow rate in the feedback loop. It is important to note, however, that the efficacy of a single-trap depends on several parameters, which include not only the flow rate of the carrier gas, but also the specific activity of the charcoal used in the trap, and the radon activity at the input of the trap. These parameters have been explored in Sec. 3 to determine the efficacy of a standalone single-trap RRS. To estimate the efficacy of a single-trap in a VSA system, Eq. (3.7a) in Sec. 3 needs to be modified to account for the input and output radon activities in a single feed cycle. Therefore, the total trap contribution A_{trap} from the charcoal, introduced in the second term in Eq. (3.7a), needs to be reduced to the contribution in a single feed cycle (given by Eq. (4.4)) according to

$$(A_{trap})_{feed} = \frac{(N_{trap})_{feed}}{\tau} = \frac{T_{feed} A_{trap}}{\tau}. \quad (\text{A.1})$$

After this modification, the efficacy of a single trap, $\epsilon_{st} = 1 - (A_{out}/A_{in})_{feed}$, can be calculated from

$$(A_{out})_{feed} = (A_{in})_{feed} e^{-\frac{mk_a}{f\tau}} + (A_{trap})_{feed}, \quad (\text{A.2})$$

and Eq. (4.4) such that,

$$(A_{out})_{feed} = (A_{in})_{feed} e^{-\frac{mk_a}{f\tau}} + \frac{T_{feed}}{\tau} \left[s_o f \frac{\tau}{k_a} \left(1 - e^{-\frac{mk_a}{f\tau}} \right) \right]. \quad (\text{A.3})$$

The right panel of Figure (16) shows the efficacy of a single-trap ($k_a = 3,000 \text{ l/kg}$ at 190K) for a range of intrinsic charcoal activities at a fixed flow rate of 50 *SLPM*. The radon activity into the single trap was computed according to Eq. (4.6b) as $A_{in} = 3.0 \text{ mBq}$ at steady state (shown in left panel), taking into account that the radon concentration in the VSA feedback loop is the same as the input radon activity into the single trap. As seen in the right panel of Fig. (16), about 14kg of charcoal with an intrinsic activity of $s_o = 0.1 \text{ mBq/kg}$ is needed to reach a 10% efficacy. It

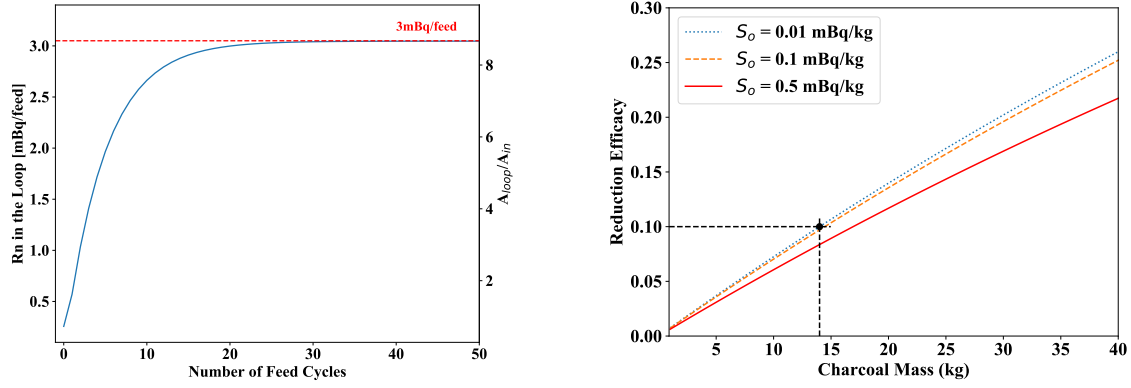


Figure 16. Left panel: Evolution of radon activity in the VSA feedback loop as a function of feed cycles. Steady state is reached after about 30 feed cycles, with an activity of 3.0mBq per feed cycle, which is 8.5 times greater than the radon activity provided by the TPC detector. Right panel: Radon reduction efficacy of single-traps with dynamic adsorption coefficients of $k_a = 3,000\text{l/kg}$ and an inlet radon activity of $A_{in} = 3.0\text{mBq}$ are shown as a function of charcoal mass for various intrinsic radon activities. The black dashed black lines indicate that about 14kg of $s_o = 0.1\text{mBq/kg}$ charcoal will give a single-trap with 0.1 efficacy in the feedback loop of the swing system.

is interesting to note though that a 10% single-trap efficacy for the same parameters can also be achieved with about 23kg of currently available Saratech charcoal (with $s_o = 0.5\text{mBq/kg}$). A general feature of a RRS efficacy is that the higher the single-trap efficacy the fewer feed cycles are needed to reach steady state, while the higher the feed column efficacy the larger the number of feed cycles are needed.

References

- [1] LZ Collaboration, D. Akerib et al., *The LUX-ZEPLIN (LZ) Technical Design Report*, arXiv:1703.09144 [physics.ins-det]
- [2] K. Pushkin et al., *Study of radon reduction in gases for rare event search experiments*, Nucl. Instrum. Meth. **A903** (2018) 267.
- [3] XENON Collaboration, S. Moriyama et al., *Direct Dark Matter Search with XENONnT*, https://www.lowbg.org/ugnd/workshop/sympo_all/201903_Sendai/slides/8am/8am_6.pdf
- [4] A. Pocar, *Low Background Techniques and Experimental Challenges for Borexino and its Nylon Vessels*, Ph.D. Thesis Princeton (2003), Report number: UMI-31-03047
- [5] J. Street et al., *Construction and Measurements of an Improved Vacuum-Swing-Adsorption Radon-Mitigation System*, AIP Conference Proceedings 1672, 150004 (2015), doi.org/10.1063/1.4928027
- [6] J. Street et al., *Radon Mitigation for the SuperCDMS-SNOLAB Dark Matter Experiment*, APS April Meeting Abstracts 2016, M16.005.
- [7] M. Arthurs, C. Amarasinghe, D. Huang, W. Lorenzon, E. Miller, CHARRS Performance in TPC Detectors (2020).
- [8] ICARUS collaboration, P. Benetti et al., *Argon purification in the liquid phase*, Nucl. Instrum. Meth. **A333** (1993) 567.

- [9] XMASS collaboration, A. Abe, et al., *Radon removal from gaseous xenon with activated charcoal*, Nucl. Instrum. Meth. **A661** (2012) 50.
- [10] Private communications with Blücher GMBH, the German producer of the Saratech brand charcoal.